A UNIFIED MODEL FOR THE SIMULATION OF SMALL-GEOMETRY DEVICES

A. Pierantoni[†], *P. Ciampolini*[*], *A. Liuzzo*[†] *and G. Baccarani*[†]

[†]Dipartimento di Elettronica, Informatica e Sistemistica - Universitá di Bologna
[*]Istituto di Elettronica - Universitá di Perugia

In the past years, fringing and proximity effects, non-stationary phenomena and device self-heating have been thoroughly, yet separately, investigated to the purpose of modeling scaled-down devices. 3D device simulators have been developed in order to cope with geometrical features, while energy transport models have been proposed to describe hot-carriers effects. Thermal phenomena were traditionally described by heuristic models, basically taking into account the plain Joule effect. Recently, more accurate "electrothermal" models were published [1,2], suitable for small structures, as well as for power devices.

The actual picture of submicron device physics, however, results from the interactions among the above effects: in this paper, the capability of the device simulator HFIELDS-3D to self-consistently describe all of them is illustrated. Such a goal is accomplished by the implementation of a generalized transport model (outlined in the following) into a versatile 3D simulation environment. The dynamic of three subsystems (electrons, holes and phonons) is described by a set of three BTEs; interactions among different subsystems are taken into account by proper collision terms.

The second-order moment of the above BTEs provides energy-balance equations for each subsystem, which read:

$$\frac{\partial W_n}{\partial t} + \operatorname{div} \vec{S}_n = \vec{F} \cdot \vec{J}_n + \left(\frac{\partial W_n}{\partial t}\right)_{coll} \quad , \quad \frac{\partial W_p}{\partial t} + \operatorname{div} \vec{S}_p = \vec{F} \cdot \vec{J}_p + \left(\frac{\partial W_p}{\partial t}\right)_{coll}$$

$$\frac{\partial W_L}{\partial t} + \operatorname{div} \vec{S}_L = \left(\frac{\partial W_L}{\partial t}\right)_{coll}$$

In the above equations, W represents the energy densities and $\vec{S}$ the energy flows, defined as follows:

$$\vec{S}_n = -\kappa_n \operatorname{grad} T_n - \left(\frac{5}{2} - s\right) \frac{k_B T_n}{q} \vec{J}_n \quad , \quad \vec{S}_p = -\kappa_p \operatorname{grad} T_p + \left(\frac{5}{2} - s\right) \frac{k_B T_p}{q} \vec{J}_p$$

$$\vec{S}_L = -\kappa_L \operatorname{grad} T_L$$

while the current densities $\vec{J}$ are given by:

$$\vec{J}_n = q\mu_n \left[\frac{k_B T_n}{q} \operatorname{grad} n + n \operatorname{grad}\left(\frac{k_B T_n}{q} - \varphi\right)\right] \quad , \quad \vec{J}_p = -q\mu_p \left[\frac{k_B T_p}{q} \operatorname{grad} p + p \operatorname{grad}\left(\frac{k_B T_p}{q} + \varphi\right)\right]$$

Finally, the collision terms are described according to the relaxation-time approximation and fulfill the following relationship:

$$\left(\frac{\partial W_L}{\partial t}\right)_{coll} + \left(\frac{\partial W_n}{\partial t}\right)_{coll} + \left(\frac{\partial W_p}{\partial t}\right)_{coll} = E_G U$$

The model is completed, as usual, by Poisson's and current-continuity equations. Discretization is carried out by the Box Integration Method, applied to the hybrid mesh suggested by Conti *et al.* [3]. The model's formulation is similar to that suggested, e.g., in [4]; previously reported simulations are limited to the works of Szeto and Reif [5] (1D), Katayama and Toyabe [6] (3D, finite differences discretization) and, more recently, Benvenuti *et al.* [7] (1D, including convective terms).

Despite the code being threedimensional, we selected a 2D device to test the code; hence, interactions with fringing effects are ruled out, and the alternative models' predictions can be more straightforwardly compared. Fig. 1 shows the simulated .3μ MOSFET. Four models are taken into account: the standard drift-diffusion (DD), the hydrodynamic model (HD), as described in [8], the electrothermal (ET) model introduced in [2] and the "generalized" thermal-hydrodynamic (TH) model illustrated so far. The electron mobility is basically described by the CVT mobility model [9], whereas the energy-dependent mobility suggested in [10] is introduced whenever the electrons average energy is available. Fig. 2 compares electron and lattice temperature profiles along the silicon upper surface, as computed by different models: they exhibit pronounced peaks at the drain junction and highlight the occurrence of both nonstationary and self-heating effects in this region. Major differences are found in the offset of the lattice temperature resulting from the ET and HT models, which are to be ascribed to the different current densities discussed below. Moreover, since no "local" relationship among the electron energy and either the electric field or the lattice temperature is assumed by the TH model, slightly smoother temperature profiles are predicted by the latter.

Further quantitative discrepancies are found in the output characteristics of Fig. 3: in the low V_{DS} range, neither carrier nor lattice heating occurs, so that predictions given by the four models agree well. At intermediate V_{DS} values, carriers may attain energies well in excess of their equilibrium values (as shown in Fig. 4), while no lattice

heating still occurs: HD and TH models consistently predict higher drain currents than DD and ET, due to the carrier velocity overshoot. Eventually the lattice heats up as well, thus resulting in increased lattice scattering probability; the $I_D^{(ET)}$ and $I_D^{(HT)}$ curves deviate downward, with respect to the corresponding isothermal models. The aforementioned effects, therefore, seem to somehow compensate themselves: in our example, the generalized model predicts a moderate deviation from the DD results, while hydrodynamic and electrothermal models respectively over- and underestimate the drain current to a non-negligible extent.

References

[1] G. K. Wachutka, *IEEE Trans. on CAD of ICAS*, vol. CAD-9, pp. 1141–1149, 1990.
[2] A. Pierantoni *et al.*, *ESSDERC'92 Proceedings*, pp. 769–772, Elsevier, 1992.
[3] P. Conti *et al.*, *IEEE Trans. on CAD of ICAS*, vol. CAD-10, pp. 1231–1241, 1991.
[4] J. Roberts and S.G. Chamberlain, *COMPEL*, vol. 9, pp. 1–22, 1990.
[5] S. Szeto and R. Reif, *Solid State Electronics*, vol. 32, no. 4, pp. 307–317, 1989.
[6] K. Katayama and T. Toyabe, *IEDM '89, Digest of technical papers*, pp. 135–138, 1989.
[7] A. Benvenuti *et al.*, *IEDM '92, Digest of technical papers*, pp. 737–740, 1992.
[8] A. Pierantoni *et al.*, *IEICE Trans. Electron.*, vol. E75-C, no. 2, pp. 181–188, 1992.
[9] C. Lombardi *et al.*, *IEEE Trans. on CAD of ICAS*, vol. CAD-7, no. 11, pp.1164-1171, 1988
[10] W. Hänsch and M. Miura-Mattausch, *J. Appl. Phys.*, vol. 60, p. 650, 1986.

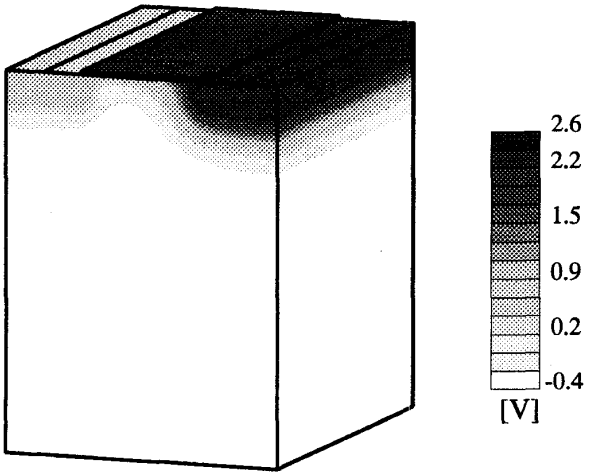

Fig. 1: View of the simulated device. The gray scale refers to the potential values ($V_{GS} = V_{DS} = 2$V).

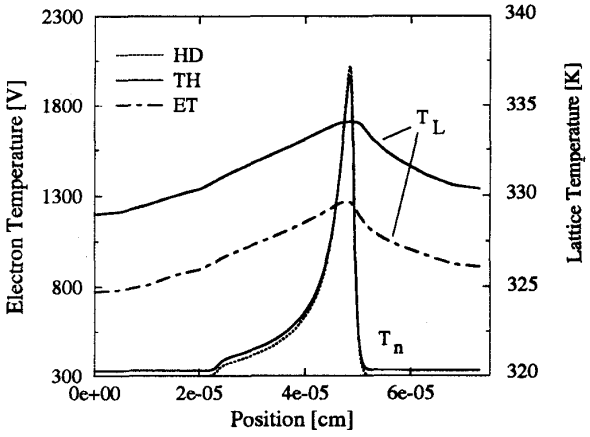

Fig. 2: Carrier and lattice temperature profiles along the device upper surface. ($V_{GS} = V_{DS} = 2$V).

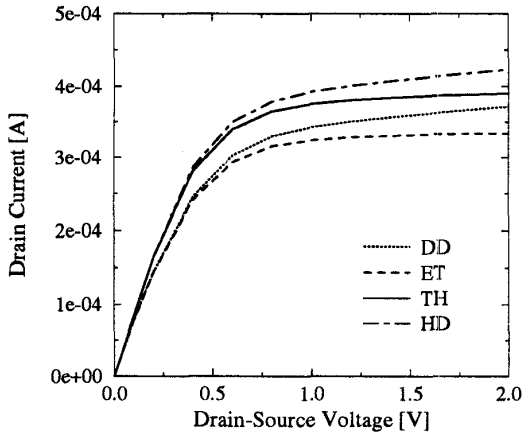

Fig. 3: Drain current comparison.

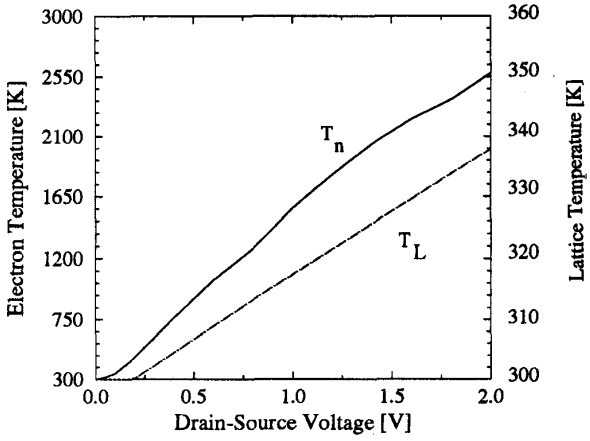

Fig. 4: Bias dependence of carrier and lattice peak temperatures.